



Seasonal dripwater Mg/Ca and Sr/Ca variations driven by cave ventilation: Implications for and modeling of speleothem paleoclimate records

Corinne I. Wong^{a,*}, Jay L. Banner^a, MaryLynn Musgrove^b

^a Jackson School of Geosciences, The University of Texas, Austin, TX 78712, USA

^b U.S. Geological Survey, Austin, TX 78754, USA

Received 20 December 2010; accepted in revised form 17 March 2011; available online 22 March 2011

Abstract

A 4-year study in a central Texas cave quantifies multiple mechanisms that control dripwater composition and how these mechanisms vary at different drip sites. We monitored cave-air compositions, in situ calcite growth, dripwater composition and drip rate every 4–6 weeks. Three groups of drip sites are delineated (Groups 1–3) based on geochemical variations in dripwater composition. Quantitative modeling of mineral-solution reactions within the host carbonate rock and cave environments is used to identify mechanisms that can account for variations in dripwater compositions. The covariation of Mg/Ca (and Sr/Ca) and Sr isotopes is key in delineating whether Mg/Ca and Sr/Ca variations are dictated by water–rock interaction (i.e., calcite or dolomite recrystallization) or prior calcite precipitation (PCP). Group 1 dripwater compositions reflects a narrow range of the extent of water–rock interaction followed by varying amounts of prior calcite precipitation (PCP). Group 2 dripwater compositions are controlled by varying amounts of water–rock interaction with little to no PCP influence. Group 3 dripwater compositions are dictated by variable extents of both water–rock interaction and PCP. Group 1 drip sites show seasonal variations in dripwater Mg/Ca and Sr/Ca, whereas the other drip sites do not. In contrast to the findings of most previous dripwater Mg/Ca–Sr/Ca studies, these seasonal variations (at Group 1 drip sites) are independent of changes in water flux (i.e., rainfall and/or drip rate), and instead significantly correlate with changes in cave-air CO₂ concentrations. These results are consistent with lower cave-air CO₂, related to cool season ventilation of the cave atmosphere, enhancing calcite precipitation and leading to dripwater geochemical evolution via PCP. Group 1 dripwater Mg/Ca and Sr/Ca seasonality and evidence for PCP as a mechanism that can account for that seasonality, have two implications for many other regions where seasonal ventilation of caves is likely: (1) speleothem trace-element records may provide seasonal signals, and (2) such records may be biased toward recording climate conditions during the season when calcite is depositing. Additionally, we use our results to construct a forward model that illustrates the types of speleothem Mg/Ca and Sr/Ca variations that would result from varying controls on dripwater compositions. The model provides a basis for interpreting paleodripwater controls from high frequency Mg/Ca and Sr/Ca variations for speleothems from caves at which long term monitoring studies are not feasible.

© 2011 Elsevier Ltd. All rights reserved.

1. INTRODUCTION

Speleothems are cave mineral deposits, and speleothem compositions are used as proxies for terrestrial Pleistocene and Holocene paleoclimate records. It is necessary to understand how variations of any proxy reflect climate in order to interpret climate records from proxies. This is

* Corresponding author. Present Address: 1 University Station – C1100, Austin, TX 78712, USA. Tel.: +1 512 963 9567; fax: +1 512 232 1913.

E-mail addresses: corinnewong@mail.utexas.edu (C.I. Wong), banner@mail.utexas.edu (J.L. Banner), mmusgrov@usgs.gov (M. Musgrove).

especially true for speleothem proxies, as the climate signal is filtered in the transit of water through the subsurface, interactions with soil and bedrock, and in the transfer of water compositions into speleothem compositions within the cave.

Assessing speleothem compositions as proxies requires consideration of the relation between (i) climate variability and dripwater compositions and drip rate, (ii) climate variability and speleothem growth, and (iii) dripwater compositions and speleothem compositions. This study uses data from a multi-year monitoring study to elucidate the controls on dripwater Mg/Ca, Sr/Ca, and $^{87}\text{Sr}/^{86}\text{Sr}$ compositions and demonstrate the relationship between climate variability and dripwater compositions. The results are used to design a forward model that illustrates the types of speleothem variations that might result from varying controls on dripwater compositions and speleothem growth. The objective of the model is to provide a basis for interpreting paleo-dripwater controls from high frequency speleothem Mg/Ca and Sr/Ca variations for speleothems that originate from caves at which long term cave and dripwater monitoring studies are not feasible due to such reasons as restricted access or absence of active dripwater.

Previous studies have discussed multiple controls on dripwater Mg/Ca and Sr/Ca. These controls include local compositional variations of soils and bedrock, the type of flow paths (i.e., conduit vs. diffuse) that supply drip sites, various types and amounts of water–rock interaction (i.e., recrystallization of calcite, recrystallization of dolomite, or incongruent dissolution of dolomite), temperature and growth-rate dependent K_D values for Mg and Sr, respectively, and variable extents of prior calcite precipitation (PCP) (Fairchild and Tremble, 2009). Note that water–rock interaction and PCP are discussed as two distinct processes in this manuscript. The amount of water–rock interaction that occurs is largely dictated by variable water residence time (i.e., the amount of time water spends in the subsurface above the cave), whereas PCP (i.e., calcite precipitation that occurs any time prior to the dripwater collection, whether on the cave ceiling or in conduits, fractures, or pores in the subsurface above the cave) can be dominantly dictated by variable water residence time or ventilation of cave-air CO_2 .

Seasonal ventilation of cave-air CO_2 and its effects on dripwater compositions and speleothem growth is a topic of growing interest. Temperature-related density differences between surface and cave air result in two end member seasons, (i) seasonal stagnation of cave air that results in a build up of cave-air CO_2 , and (ii) seasonal ventilation that results in a reduction of cave-air CO_2 (Banner et al., 2007; Kowalczyk and Froelich, 2010). Seasonally high (or low) cave-air CO_2 concentrations limit (or enhance) CO_2 degassing from cave dripwater and hinder (or promote) calcite precipitation, which results in seasonal variations in speleothem growth rates (Banner et al., 2007; Baldini et al., 2008) and development of physical speleothem lamina (Boch and Spotl, 2008). Seasonal variations in calcite growth result in seasonal variations of PCP, which in turn results in seasonal variations in drip-water $\delta^{13}\text{C}$ of dissolved inorganic carbon (Spotl et al., 2005; Guilfoyle, 2006) and Mg/Ca

and Sr/Ca (Mattey et al., 2010). Annual variations in speleothem $\delta^{13}\text{C}$ have also been interpreted as reflecting seasonal ventilation (Jo et al., 2010).

Seasonal variations in dripwater and speleothem Mg/Ca and Sr/Ca have alternatively been interpreted as reflections of seasonal variations in rainfall (Johnson et al., 2006; McDonald et al., 2007). Rainfall variations influence both the water residence time and the degree of water saturation of the subsurface above the cave, both of which can be reflected in dripwater Mg/Ca and Sr/Ca values. The amount of water residence time dictates the amount of water–rock interaction that occurs, with drier intervals resulting in longer residence time, more extensive water–rock interaction and higher Mg/Ca and Sr/Ca (Musgrove and Banner, 2004). The degree of saturation of the subsurface above the cave determines the amount of ventilation and the extent to which PCP can occur, with drier intervals resulting in more ventilation, greater extents of PCP, and higher Mg/Ca and Sr/Ca (Karmann et al., 2007; McDonald et al., 2007). It has also been proposed that drier intervals result in slower drip rates within the cave, which allows for more PCP to occur (Johnson et al., 2006). Note that varying amounts of both water residence time and PCP result in higher Mg/Ca and Sr/Ca during drier conditions, and Mg/Ca and Sr/Ca variations alone cannot be used to distinguish between the processes. Additionally, Mg/Ca and Sr/Ca variations alone cannot be used to distinguish between seasonal cave ventilation and seasonal rainfall variations in areas where seasonal rainfall corresponds with intervals of limited cave ventilation. This is because both processes would result in lower Mg/Ca and Sr/Ca.

Sr isotope variations can theoretically be used to distinguish between changes in dripwater Mg/Ca and Sr/Ca caused by variations in water–rock interaction and PCP. $^{87}\text{Sr}/^{86}\text{Sr}$ values can be used to track relative extents of water–rock interaction in settings where overlying soils have Sr isotope compositions distinct from the host carbonate bedrock (Banner et al., 1996; Musgrove and Banner, 2004). Dripwater evolution via water–rock interaction results in the covariation of $^{87}\text{Sr}/^{86}\text{Sr}$ values and Mg/Ca and Sr/Ca. PCP, however, should not alter the $^{87}\text{Sr}/^{86}\text{Sr}$ value of the dripwater because fractionation of Sr isotopes is negligible (Banner and Kaufman, 1994). Therefore, invariant $^{87}\text{Sr}/^{86}\text{Sr}$ values that coincide with changes in Mg/Ca and Sr/Ca would be indicative of PCP as opposed to water–rock interaction.

This study presents the results from a multi-year cave monitoring study in central Texas. We monitored Mg/Ca, Sr/Ca, and $^{87}\text{Sr}/^{86}\text{Sr}$ at nine drip sites at relatively high temporal resolution – every 4–6 weeks – over a 4-year time period. The results are used with quantitative modeling to delineate the multiple mechanisms and their relative controls on dripwater composition at different drip sites within a single cave. Our research builds on previous studies at Natural Bridge Caverns that identified diagnostic geochemical differences between soils and limestones and provided insight on mineral-solution reactions and flow paths that may control dripwater evolution (Musgrove and Banner, 2004). Controls on dripwater $\delta^{18}\text{O}$ and $\delta^{13}\text{C}$ have also been previously assessed in this cave system (Pape et al., 2010;

Guilfoyle, 2006). We find seasonal variations in dripwater Mg/Ca and Sr/Ca, and use the covariation of Mg/Ca, Sr/Ca, and $^{87}\text{Sr}/^{86}\text{Sr}$ values to constrain the processes responsible for these fluctuations. We use the results to create a forward model that illustrates how high frequency speleothem Mg/Ca and Sr/Ca records might be used to interpret controls on paleo-dripwater.

2. HYDROGEOLOGIC SETTING

Dripwaters were sampled in Natural Bridge Caverns in central Texas at depths of 30–60 m (Fig. 1). The cave is developed in the Edwards Plateau, which is a regionally extensive karstified Cretaceous carbonate platform (Maclay and Small, 1983). The study area is within the recharge zone of the Edwards-Trinity aquifer and the contributing zone of the Edwards aquifer. The hydrogeology and geomorphology of the area is discussed by Elliott and Veni (1994).

Natural Bridge consists of two adjacent caves (South and North) formed in the cavernous layer of the upper Glen Rose Formation and the bottom part of the Krainer Formation (Small and Hanson, 1994). The cave has a lateral extent of 1160 m and a maximum depth of 75 m (Elliott and Veni, 1994). Higher cave-air CO_2 concentrations occur in the South Cave than in the North Cave during the summer months, but similar concentrations are observed in both caves during the winter (Wong and Banner, 2010). Within each cave, CO_2 concentrations are generally similar throughout the main passages of the caves. Two sample sites in the South Cave, however, commonly have higher concentrations relative to the other sites, which might be controlled by differences in the spatial distribution of fractures and solution widened-conduits that allow focused advection or diffusion of CO_2 from the soil zone (Wong and Banner, 2010). Seasonal variations in cave-air CO_2 have been documented in both caves, which is attributed

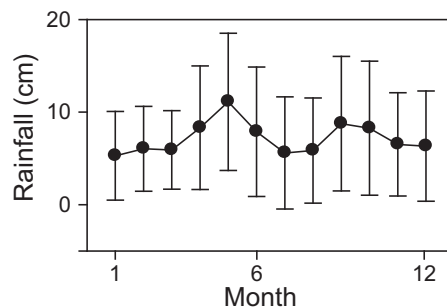


Fig. 2. Monthly rainfall average and variability is shown for San Antonio, Texas. Average monthly rainfall is shown with error bars illustrating one standard deviation, and is based on a rainfall record from 1856 to 2008. Data was retrieved from the National Weather Service Forecast Office for San Antonio, TX, (<http://www.srh.noaa.gov/ewx/?n=satclidata.htm>).

to density-driven ventilation of cave air by surface air during the winter season when surface air is cooler (and therefore denser) than cave air (Banner et al., 2007).

The site is located where the climate regime transitions from sub-humid to semi-arid, and average annual rainfall is 740 mm and ranges from 250 to 1320 mm (1856–2008). The rainfall climatology demonstrates a tendency for greater rainfall amounts in the fall and spring. There is, however, large interannual variability, as average rainfall for 1 month is within one standard deviation of every other month (Fig. 2). The large interannual rainfall variability is exemplified during the period of study as the amount and timing of rainfall is inconsistent year to year. The surface above the caves is covered with thin (<30 cm) clay-rich mollisols and juniper, oak, savanna grasses, and cacti (Cooke et al., 2007). A portion of the North Cave is covered with urban infrastructure associated with the cavern's commercial visitor center.

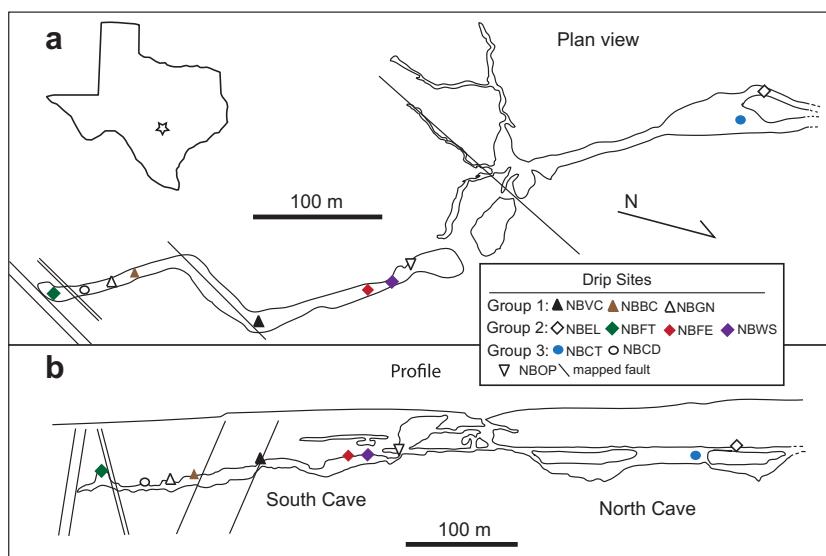


Fig. 1. Plan (a) and profile (b) map of the North and South caves that comprise Natural Bridge Caverns (located in central Texas) along with drip sites where drip-water and cave-air CO_2 , temperature, and relative humidity were monitored. Calcite growth was measured at NBCT, NBWS, and NBOP. Dripwater was not monitored at NBOP. The plan and profile maps are simplified from Elliott and Veni (1994).

3. METHODS

Nine drip sites were visited every 4–6 weeks from May 2004 to April 2008 to collect water samples and measure physical parameters (drip rate and cave-air CO₂, temperature, and relative humidity). Higher-resolution logging of drip rate was conducted at three sites using Rainwise tipping buckets wired to Onset Microstation dataloggers. Cave-air CO₂ and temperature were measured at each site with a handheld TelAire 7001 CO₂ meter ($\pm 5\%$), and relative humidity was measured using a Extech RH 355 psychrometer. Pre-cleaned polypropylene sample bottles (not acid washed) were left for 1–3 h to collect dripwater. Bottles were collected from the cave and aliquots were poured into acid-cleaned polypropylene sample bottles (and acidified with ultra-pure concentrated nitric acid) for cation and strontium isotope analyses. When there were sufficient volumes of water, water temperature, pH, and conductivity were measured using a Myron L Company Ultrameter II, and any remaining water was aliquoted into non-acid-cleaned polypropylene bottles for anion analysis and amber glass vials with no head space for alkalinity analyses. Alkalinity analyses were conducted within 24 h of collection using an autotitrator to an endpoint of pH 4.5.

Drip sites are spatially distributed throughout the North and South Cave (Fig. 1). Drip site overburden varies from ~ 30 to 60 m, drip height ranges from 0.3 to 10 m, and some drip sites are located adjacent to mapped faults (Table 4A). Drips fall from a variety of formations (soda straws, cave bacon, chandeliers, flowstone, fin-shaped draperies) onto a variety of formations (fried egg stalagmites, flowstone, flat platforms, stubby, symmetrical stalagmites, cone-shaped cratered stalagmites). It appears that calcite is actively being precipitated below all but two of the sampled drip sites based on visual inspection. Calcite growth has previously been measured under three of the sites (NBCT, NBWS, and NBOP), and observed to have seasonal variation in growth rates with higher growth rates in the winter and slower growth rates in the summer (Banner et al., 2007). Calcite growth has been observed on monitoring equipment left under the drip at two additional sites (NBBC and NBFT).

Modern calcite was collected on glass plates that were placed horizontally under three drip sites (NBCT, NBWS, and NBOP). Monitoring calcite growth at these sites builds on the data set presented by Banner et al. (2007); there is no drip-water data for one of these sites due to its extremely low drip rate and therefore limited water volume (NBOP). Plates were retrieved every 4–6 weeks, and weighed using a Sartorius MC1 RC 210P electronic balance following the methods described by Banner et al. (2007). The amount of calcite deposition was determined from the difference in plate weight before and after collection. Standard deviation of the repeatedly weighed standard is 0.0003 g prior to August 2007, 0.002 g (0.3–10% of median values) from August to November 2007, and 0.0002 g following November 2007. For reference, calcite deposition from all sites ranged from below detection limit (0.0003 g) to 4.84 g with a median value of 0.03 g.

Rainfall data was measured using an on-site rain gauge, and supplemented by data from a nearby (10 km) U.S. Geological Survey site (site no. 08167347) from 08/23/07 to 11/25/07 when the on-site rain gauge was not functioning. Daily surface weather data (temperature, barometric pressure, and relative humidity) was obtained from a nearby NOAA station (Canyon Dam, COOP-ID 411429) and supplemented by data from another station (New Braunfels, COOP-ID 416276), from 1/1/06 to 6/1/06, when the prior station was not reporting.

Daily surface and cave air density, ρ , was estimated using $\rho = [P^*(1 + XM)]/[0.28703^*T^*(1 + 1.16078^*XM)]$, where P is barometric pressure in kPa, T is temperature in Kelvin, and XM is the mixing ratio. The mixing ratio is approximated using $XM = 0.622^*VP/(P - VP)$, where $VP = RH^*SVP/100$, $SVP = 0.61121^*e^{[17.67^*T/(T+243.5)]}$, and RH is relative humidity. These equations are appropriate for calculating the density of humid air, similar to the equations used to calculate surface and cave air densities in a previous study (James and Banner, 2009; Kowalczyk and Froelich, 2010). Daily cave temperature and relative humidity data were linearly interpolated from measurements made every 4–6 weeks. Barometric pressure was not measured in the cave, so surface barometric pressure values are used. While this is a limitation in the estimation of cave air density, the effects are likely small because (i) variations in surface and cave air measurements have been shown to be near synchronous on a seasonal scale (Genty and Deflandre, 1998) and (ii) seasonal cave ventilation is linked with surface and cave air temperature differences as opposed to pressure differences (Spotl et al., 2005; Banner et al., 2007; Baldini et al., 2008). Density differences between surface and cave air density and corresponding changes in cave air CO₂ are used as a proxy for cave ventilation as done previously (Banner et al., 2007; Baldini et al., 2008).

Soils were collected from the surface above drip sites and leached in ammonium acetate to obtain the cation-exchangeable fraction. Limestone samples were collected from the surface and within the cave and weathered surfaces were removed. Samples were partially dissolved in acetic acid after being leached with ammonium acetate.

Geochemical analyses were conducted in the Department of Geological Sciences at UT-Austin. For cation analysis, samples were diluted 1:10 with 2% HNO₃, and measured using an Agilent 7500ce quadrupole ICP-MS. Machine drift is compensated for by mixing with an internal standard solution of Sc, Y, Ho, and Tm. Analytical uncertainty based on the RSD of 12 analyses of external water standards (NIST 1640 and 1643e) for Ca, Mg, and Sr is 10%, 8%, and 6%, respectively, and for Mg/Ca and Sr/Ca is 6% and 9%, respectively. Average percent difference between measured and actual values for the standards is 12%, 4%, and 3% for Ca, Mg, and Sr. Analytical uncertainty based on the average percent difference of 16 replicate unknown water samples for Mg/Ca and Sr/Ca is 6% and 8%, respectively. Strontium isotope ratios were measured dynamically using a multi-collector Finnigan-MAT 261 thermal ionization mass spectrometer, following methods in Banner and Kaufman (1994). The mean ⁸⁷Sr/⁸⁶Sr value for NIST SRM 987 measured during the study was

Table 1
Median (ranges) concentrations of Mg/Ca, Sr/Ca, and $^{87}\text{Sr}/^{86}\text{Sr}$.

	Mg (ppm)	Sr (ppm)	Ca (ppm)	Mg/Ca (mol/mol)	Sr/Ca (mmol/mol)	$^{87}\text{Sr}/^{86}\text{Sr}$
<i>Drip-water</i>						
Group 1	28 (14–34)	0.09 (0.07–0.17)	47 (16–87)	0.95 (0.38–2.45)	0.85 (0.51–1.88)	0.70839 (0.70833–0.70841 [*])
Group 2	4.2 (2–10)	0.05 (0.03–0.07)	112 (46–155)	0.08 (0.01–0.26)	0.20 (0.07–0.43)	0.70893 (0.70879–0.70907)
Group 3	9 (7–17)	0.06 (0.05–0.10)	60 (29–109)	0.24 (0.22–0.69)	0.42 (0.26–0.84)	0.70885 (0.70881–0.70896)
Soil leachate				0.04 (0.04–0.06)	0.21 (0.19–0.28)	0.70911 (0.70906–0.70917)
Limestone	3570 (2050–6060)	51 (13–73)		0.009 (0.005–0.015)	0.13 (0.03–0.31)	0.70768 (0.70755–0.70787)

* This range excludes a single measurement of 0.70874 ($n = 41$ for this group).

0.710261 ($2\sigma = 0.000014$, $n = 56$). Replicate $^{87}\text{Sr}/^{86}\text{Sr}$ analyses on eight unknowns are within 0.000010. Procedural blank values are 17–25 pg for Sr isotope measurements of dripwater and carbonate rock, and are negligible with respect to the typical sample size of 200 ng Sr. The procedural blank value for the soil leachate procedure is 950 pg, which represents 0.45% of the amount of Sr used for the analysis. The quantity of the blank, however, is insignificant when comparing values from soils to those of dripwater and limestone samples.

4. RESULTS

4.1. Drip-water, soil and carbonate rock compositions

Elemental concentrations, Mg/Ca, Sr/Ca, and $^{87}\text{Sr}/^{86}\text{Sr}$ values for waters, soil leachates and carbonate rocks are summarized in Table 1. Dripwaters are Ca–HCO₃ (pH 6.8–8.3) waters, and have $^{87}\text{Sr}/^{86}\text{Sr}$ values ($^{87}\text{Sr}/^{86}\text{Sr} = 0.7083$ –0.7091) that range between values for carbonate rocks (0.7076–0.7079) and soil leachates (0.7091–0.7092). $^{87}\text{Sr}/^{86}\text{Sr}$ values and Mg/Ca and Sr/Ca for these samples are similar to those for samples previously collected at Natural Bridge (Musgrove and Banner, 2004; Mihealsick et al., 2004). Detailed geochemical data for dripwater, soil, and limestone compositions are given in Tables 1A–3A.

Drip sites were classified into three groups based on geochemical differences in the ranges of Ca, Mg, and Sr concentrations and Mg/Ca, Sr/Ca, and $^{87}\text{Sr}/^{86}\text{Sr}$ values between drip sites (Table 1). Group 1 ($n = 3$) dripwaters

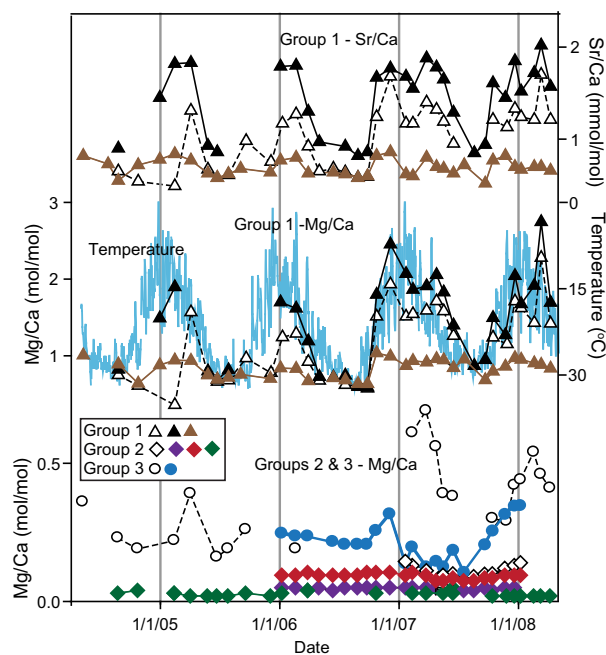


Fig. 3. Time series of surface air temperature and drip-water Mg/Ca and Sr/Ca dripwater Mg/Ca and Sr/Ca are shown for all Group 1 drip sites, and Mg/Ca is shown for Groups 2 and 3 drip sites. The surface air temperature time series is shown on an inverted scale.

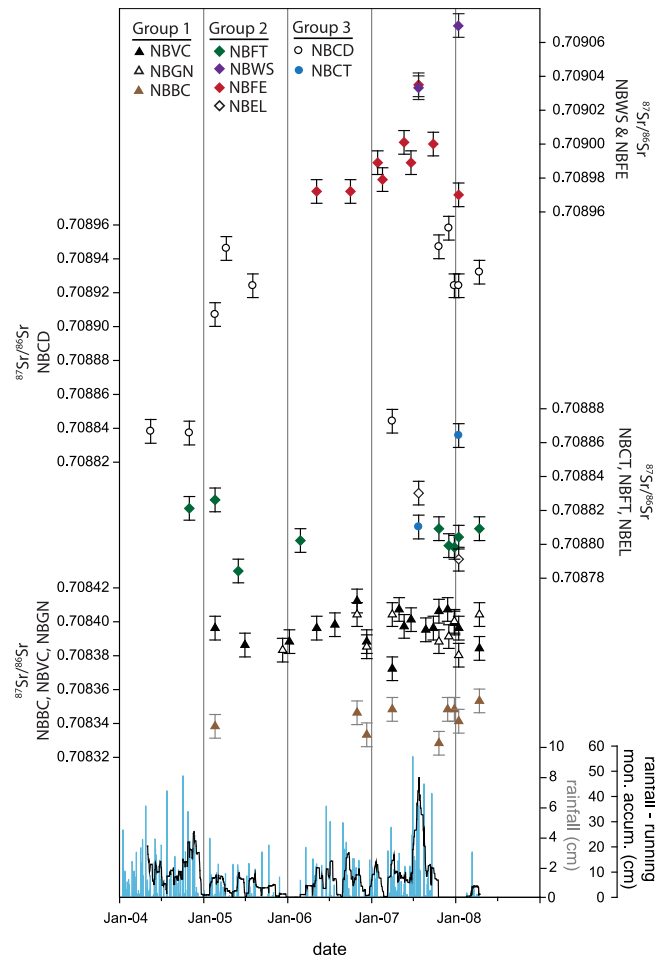


Fig. 4. Dripwater $^{87}\text{Sr}/^{86}\text{Sr}$ time series for each drip site. Note the variable scales for $^{87}\text{Sr}/^{86}\text{Sr}$ values. Daily rainfall (blue bars) and monthly-accumulated rainfall (black line) is also shown. Note that Group 1 drip sites have lower $^{87}\text{Sr}/^{86}\text{Sr}$ values that are less variable relative to Groups 2 and 3 drip sites. (For interpretation of the references to colors in this figure legend, the reader is referred to the web version of this paper.)

have high Mg/Ca, Sr/Ca (Fig. 3), and Mg and Sr concentrations, low $^{87}\text{Sr}/^{86}\text{Sr}$, and low Ca concentrations relative to Group 2 ($n = 4$) dripwaters. Group 3 ($n = 2$) dripwaters have Mg/Ca and Sr/Ca and Mg, Sr, and Ca concentrations that are in between Groups 1 and 2, and $^{87}\text{Sr}/^{86}\text{Sr}$ values similar to Group 2. Group 1 exhibits markedly consistent $^{87}\text{Sr}/^{86}\text{Sr}$ values over a large range of Mg/Ca and Sr/Ca, while Groups 2 and 3 drip waters exhibit a wide range of $^{87}\text{Sr}/^{86}\text{Sr}$ relative to Mg/Ca and Sr/Ca (Table 1 and Fig. 4). There are no obvious, systematic differences between the groups, which are geochemically defined, with regard to other drip site features such as the location within the cave, type of formations that drips are falling from or onto, drip height, amount of overburden, or presence or absence of active calcite growth. Drips from Groups 1 and 3, however, generally fall from larger ceiling formations than Group 2 (Table 4A).

4.2. Hydrogeologic relationships

Based on monthly drip rate measurements, Group 1 drip sites have low maximum drip rates (0.74–10.9 ml/min) and

a low drip-rate coefficient of variation (0.36–0.52). Group 2 sites and one site from Group 3 have high maximum drip rates (48–813 ml/min) and a high coefficient of variation (1.18–2.02). A second site in Group 3 has a low maximum drip rate (1.56 ml/min), but a high coefficient of variation (1.56). Drip-rate characteristics of Group 1 (low drip rate maximum and drip rate variability) indicate that diffuse (seepage) flow paths supply these drip sites (Smart and Friederich, 1986; Baldini et al., 2006). Diffuse flow paths are tortuous, slow to respond or unresponsive to rain events, supply a slow and steady drip rate, and dictate relatively long water residence times. Groups 2 and 3, with high drip rate maximum and drip rate variability, are dominantly supplied by conduit flow paths. Conduit flow drip sites have more direct connections to the surface, are responsive to rain events, supply a fast and inconsistent drip rate, and are associated with short water residence times.

Drip site classifications as diffuse vs. conduit are also consistent with continuously monitored drip rate data from three sites (NBBC, NBVC, and NBFT). Diffusely classified drip sites (NBBC and NBVC) have constant drip rates even

Table 2

Number and R^2 of significant ($p < 0.05$) correlations between dripwater compositions and physical parameters.

Group	n	Rainfall – DR ^a	DR – Mg/Ca ^b	DR – ⁸⁷ Sr/ ⁸⁶ Sr ^a	CO ₂ – Mg/Ca ^c	Mg/Ca – Sr/Ca ^a	Mg/Ca – ⁸⁷ Sr/ ⁸⁶ Sr ^b
1	3	0	0	0	3 (0.50–0.90)	3 (0.56–0.95)	0
2	4	4 (0.40–0.76)	3 (0.43–0.53)	1 (0.72)	0	3 (0.64–0.91)	3 (0.44–0.86)
3	2	0	0	1 (0.64)	1 (0.57)	2 (0.86–0.91)	0

DR = monthly sampled drip rate, Temp = surface air temperature, CO₂ = cave air [CO₂]. Correlations with Sr/Ca are not shown because Mg/Ca strongly correlates with Sr/Ca.

^a Positive linear correlation.

^b Negative linear correlation.

^c Inverse correlation.

following large rain events (Fig. 1A). The conduit-classified site (NBFT) has variable drip rates that nearly cease during dry intervals and are extremely high following large rain events.

The drip sites exhibit variable relationships between (a) rainfall and drip rate and (b) measures of water flux (i.e., rainfall and drip rate) and drip-water compositions (i.e., Mg/Ca, Sr/Ca, ⁸⁷Sr/⁸⁶Sr). Group 1 has the fewest and weakest correlations between the above pairs of parameters, Group 2 has the most abundant and strongest correlations, and Group 3 is intermediate (Table 2). The lack of correlations between Group 1 drip rate and rainfall

(Table 2 and Fig. 5) and dripwater compositions and measures of water flux (Fig. 6) indicate that variability in Group 1 water compositions is not dominantly controlled by variations in water flux. The presence of correlations between dripwater compositions and measures of water flux at Groups 2 and 3 drip sites (Table 2) suggests that variations in dripwater compositions might be influenced by variations in water flux. The drip site classifications of Group 1 as diffuse and Groups 2 and 3 as conduit is consistent with the absence and presence, respectively, of correlations between measures of water flux and dripwater compositions.

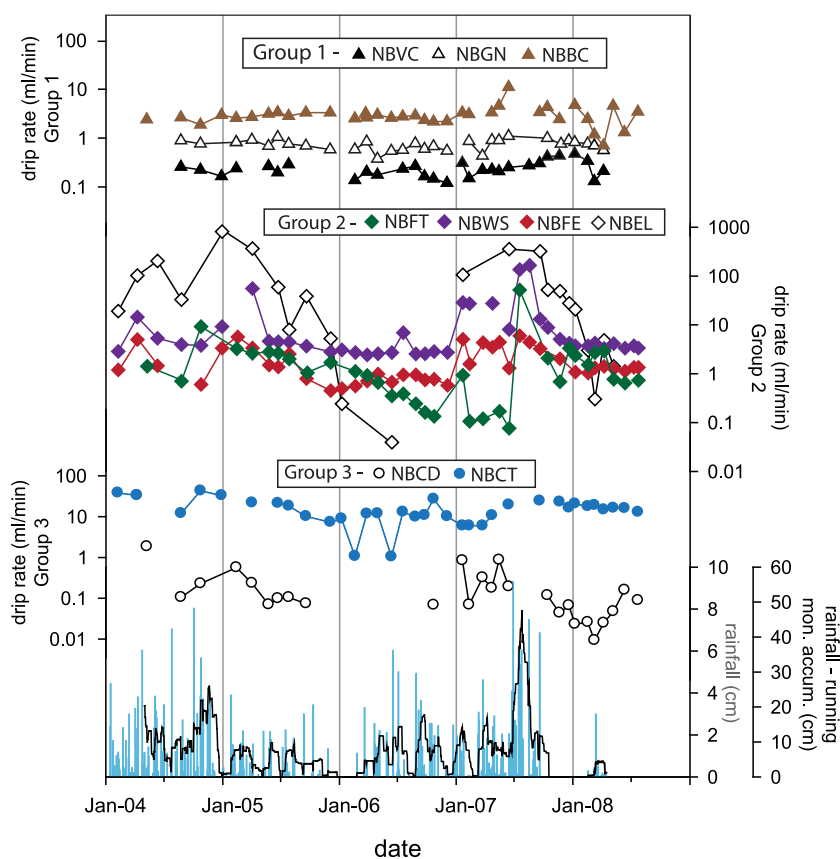


Fig. 5. Time series of drip rate for each drip site, shown by associate group (Groups 1–3). Note that drip rate is shown on a log scale. Time series for daily rainfall (blue bars) and monthly-accumulated rainfall (black line) are also shown. (For interpretation of the references to colors in this figure legend, the reader is referred to the web version of this paper.)

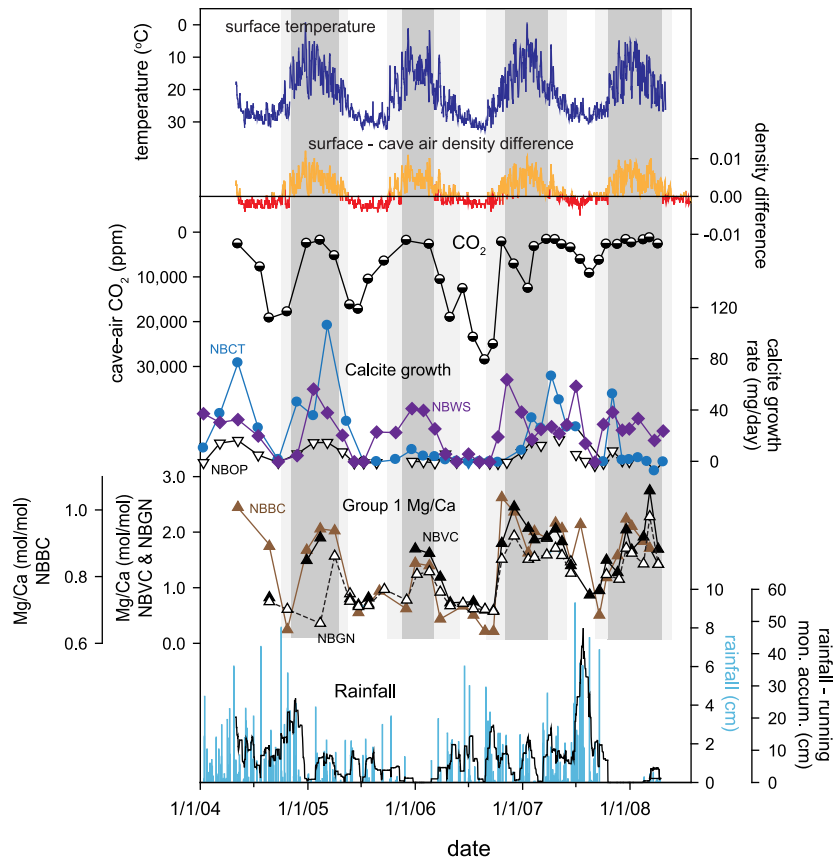


Fig. 6. Time series for Group 1 dripwater Mg/Ca, daily and accumulated (30 day) rainfall, average cave-air CO₂ (plotted inverse on log scale) from Group 1 sites, plate calcite growth rates, surface-cave air density difference, and surface air temperature (inverted scale). Density difference time series is calculated by subtracting cave air density from surface air density. Dark gray time intervals represent when surface air is denser than cave air, and light gray intervals represent transitional periods between when surface air density is less than cave air and when surface air is denser than cave air. Plate growth was measured at Groups 2 (purple) and 3 (blue) drip sites as well as at the site without dripwater data (white; scaled by an order of 10). Plate calcite growth data from 2007 to 2008 are from this study; data from 2004 and 2006 was published in Banner et al. (2007). (For interpretation of the references to colors in this figure legend, the reader is referred to the web version of this paper.)

4.3. Temporal variation in cave-air CO₂, dripwater compositions, and plate calcite growth rate

At the nine drip sites, cave-air CO₂ ranged from 380 to 37,000 ppm, and varied seasonally with a cool season (NDJF) average of 2300 ppm and a warm season (JJAS) average of 13,500 ppm. The data includes the results for this cave from Banner et al. (2007) and Cowan (2010), for which similar seasonal trends were found in this and other caves in the region. An inverse relationship exists between cave-air CO₂ and calcite growth rates on substrates in these caves (Banner et al., 2007; this study).

Group 1 sites exhibit consistent seasonal variation in Mg/Ca and Sr/Ca (Figs. 3 and 6) and both Mg/Ca and Sr/Ca exhibit significant inverse correlations with cave-air CO₂ ($p < 0.05$) and negative linear correlations with surface air temperature (Table 2). Mg/Ca and Sr/Ca are higher in the cool season when surface air is denser than cave air and cave-air CO₂ is lower, and lower in the warm season when surface air is less dense than cave air and cave-air CO₂ is higher. Interannual variability of cool season Mg/Ca and Sr/Ca maxima are also observed (Fig. 6). Group

2 sites do not exhibit consistent seasonal variations or correlation with cave-air CO₂ or temperature (Fig. 3 and Table 2). Group 3 sites exhibit subdued seasonal variation, no correlation with temperature, and inconsistent correlations with cave-air CO₂ (Fig. 3 and Table 2).

Plate calcite growth rates measured as part of this study in 2007–2008 are consistent with plate calcite growth rates reported by Banner et al. (2007) for 2004–2006 (Fig. 6). Growth rates are higher during winter intervals and lower during summer intervals. All three plate sites show large interannual variability. The relative growth rate of one site (NBOP) is consistently an order of magnitude lower than those of the other two sites due to a much lower growth rate (Banner et al., 2007). Relative growth rate between the two faster growing sites, however, is inconsistent from year to year.

5. DISCUSSION

The physical (drip rate) and geochemical (Mg/Ca, Sr/Ca, ⁸⁷Sr/⁸⁶Sr, and Ca, Mg, and Sr concentrations) parameters that define the drip-site Groups 1–3 are also indicative

of the processes that control dripwater compositions at those sites. We discuss here the processes delineated by considering multiple parameters of each drip site, including (1) type of supplying flow path, (2) dripwater elemental and isotopic covariations, and (3) seasonal variation of dripwater Mg/Ca and Sr/Ca. Quantitative modeling of vadose zone processes of water–rock interaction and prior calcite precipitation (PCP) allow us to constrain the nature of these processes and the sequence in which they occur in the geochemical evolution of Groups 1–3 waters. Recall that we define water–rock interaction as the recrystallization (i.e., dissolution and re-precipitation) of calcite or dolomite within the host rock, and discuss it as a process distinct from PCP that occurs on the cave ceiling or in pores and fractures connected to the cave (Fig. 7).

5.1. Covariation of Mg/Ca, Sr/Ca and $^{87}\text{Sr}/^{86}\text{Sr}$ values

Vadose water in central Texas karst acquires its initial Mg/Ca, Sr/Ca, and Sr isotope signature from the soil through which it infiltrates. Rainwater has low concentrations of Mg (mean = 0.12 ± 0.12 ppm; National Atmospheric Deposition Program Monitoring Location TX03) and Sr (mean = 5.6 ± 8 ppb, $n = 4$; Oetting, 1995; Musgrove and Banner, 2004) relative to the most dilute dripwater concentrations (Mg = 1.5 ppm; Sr = 40 ppb), indicating that dripwater acquires most of its Mg and Sr from interaction with the soil and limestone host rocks that it moves through. As water subsequently infiltrates through and reacts with host carbonate rocks, it attains higher Mg/

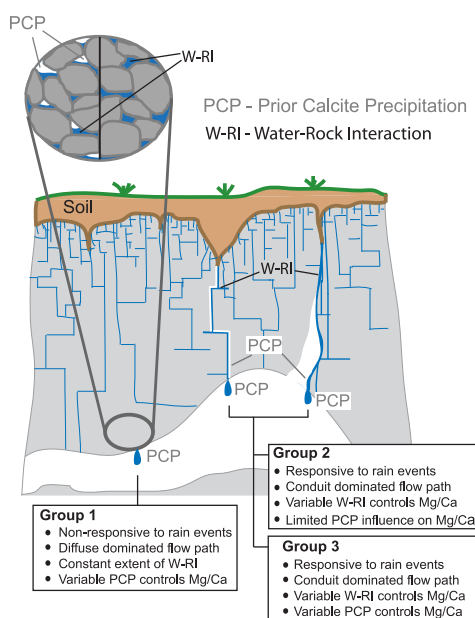


Fig. 7. Conceptual diagram illustrating the controls on drip-water compositions. WR-I occurs as water infiltrates through the subsurface prior to entering the cave. PCP occurs on the ceiling of the cave and in the pores, fractures, and conduits in the subsurface above the cave. Dripwater Mg/Ca (and Sr/Ca) variability is affected by WR-I, PCP, or a combination of WR-I and PCP.

Ca and Sr/Ca and lower $^{87}\text{Sr}/^{86}\text{Sr}$ values (Musgrove and Banner, 2004). Progressive carbonate mineral dissolution results in decreasing $^{87}\text{Sr}/^{86}\text{Sr}$ values of water, tracking the shift from a soil source to a Cretaceous carbonate rock source of Sr (Fig. 8a inset). Whereas water–rock interaction results in the covariation of Mg/Ca (and Sr/Ca) and $^{87}\text{Sr}/^{86}\text{Sr}$ values, prior calcite precipitation (PCP) does not alter $^{87}\text{Sr}/^{86}\text{Sr}$ values and only affects Mg/Ca and Sr/Ca values. Sr isotopes are therefore useful for discriminating between the processes of water–rock interaction and PCP.

Musgrove and Banner (2004) used modeling of dripwater evolution during mineral–solution reactions to demonstrate that water–rock interaction could account for the trend from low to high Mg/Ca and Sr/Ca and high to low $^{87}\text{Sr}/^{86}\text{Sr}$ values exhibited by dripwater from several central Texas caves. This modeling approach was applied to this data set to determine if (i) recrystallization of calcite, (ii) recrystallization of dolomite, or (iii) a combination of water–rock interaction (i.e., calcite/dolomite recrystallization) and prior calcite precipitation (PCP) could account for the dripwater compositions observed in the present study (Fig. 8). The modeling results indicate that (1) variability in soil leachate compositions and water–rock interaction can account for Groups 2 and 3 dripwater compositions with relatively low Mg/Ca and Sr/Ca, and (2) both water–rock interaction and PCP processes are required to account for Groups 1 and 3 dripwater compositions with relatively higher Mg/Ca and Sr/Ca (Fig. 8a and c). The near vertical trend of Group 1 Mg/Ca and Sr/Ca at a given $^{87}\text{Sr}/^{86}\text{Sr}$ value is strong evidence that PCP increased dripwater Mg/Ca and Sr/Ca following a constant amount of water–rock interaction that exceeds the amounts of water–rock interaction of Groups 2 and 3 dripwater (Fig. 8).

Calcite precipitation was modeled using compositions selected from model water–rock interaction curves (points G1 and G3; Fig. 8), demonstrating that Groups 1 and 3 dripwaters evolved via PCP from distinct starting compositions. Note that multiple PCP model lines starting from various points along the water–rock interaction curve (with similar Mg/Ca and Sr/Ca, but varying $^{87}\text{Sr}/^{86}\text{Sr}$ values) are required to account for all Group 3 dripwater compositions, which suggests that Group 3 dripwater experiences varying amounts of water rock interaction. Model PCP curves show good correspondence with observed trends of increasing Mg/Ca and Sr/Ca with decreasing Ca (Fig. 8b and d).

Observed Sr/Ca values of one of the Group 1 sites exhibits higher Sr/Ca values during summer conditions than what the model PCP curves can account for (NBVC-black triangles, Fig. 8d). Deviations of observed Mg/Ca and Sr/Ca from model PCP compositions in other cave systems have been previously explained as (1) resulting from PCP occurring from water that had dissolved fossil speleothem calcite, which caused lower values due to lower Mg and Sr concentrations of the dissolved material, and (2) resulting from increased contribution of water from the soil zone, which results in higher values due to higher Mg and Sr concentrations of soils (McDonald et al., 2007). Neither of these explanations are sufficient to account for higher Sr/

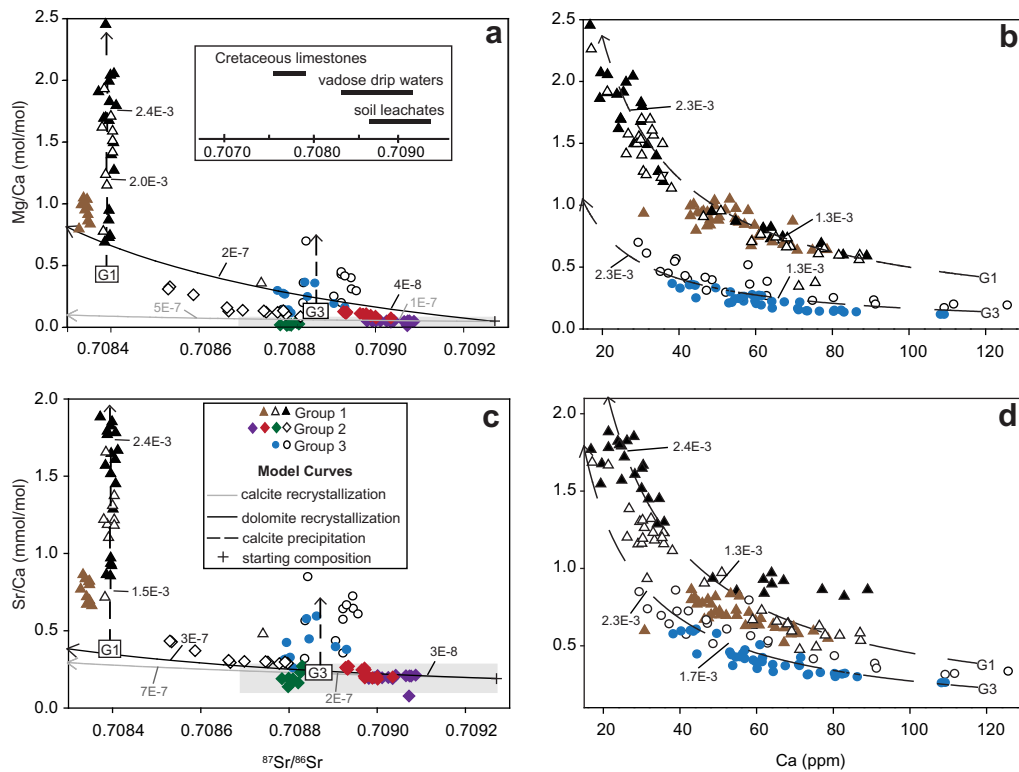


Fig. 8. Observed and modeled drip-water (a) Mg/Ca vs. $^{87}\text{Sr}/^{86}\text{Sr}$ values, (b) Mg/Ca vs Ca, (c) Sr/Ca vs. $^{87}\text{Sr}/^{86}\text{Sr}$ values, and (d) Sr/Ca vs. Ca. Shaded boxes represent the ranges of Mg/Ca, Sr/Ca, and $^{87}\text{Sr}/^{86}\text{Sr}$ values for soil leachates sampled from the surface at NB (this study; Mihealsick et al., 2004; Musgrove and Banner, 2004). Model water–rock interaction curves illustrate the geochemical changes that occur with the progressive recrystallization of calcite and dolomite in diagrams a and c, and calcite precipitation in a–d. For diagrams a and c, the initial water compositions are represented by plus signs, and consist of Mg = 3.5 mg/L, Sr = 0.05 mg/L, Ca = 120 mg/L, Mg/Ca = 0.05 mol/mol, Sr/Ca = 0.19 mmol/mol, and $^{87}\text{Sr}/^{86}\text{Sr}$ = 0.7092. Model rock composition is $^{87}\text{Sr}/^{86}\text{Sr}$ = 0.7076, Mg = 3500 ppm, Sr = 50 ppm, and stoichiometric Ca for calcite recrystallization; and $^{87}\text{Sr}/^{86}\text{Sr}$ = 0.7076, Sr = 150 ppm, and stoichiometric Ca and Mg for dolomite recrystallization. Increasing water–rock interaction is indicated by arrows and water/rock ratios (e.g., $1\text{E}-5$). Calcite precipitation is modeled subsequent to water–rock interaction, and moles of calcite precipitated are marked along the curve (e.g., $2\text{E}-3$). For graphs b and d, initial compositions, G1 and G3, are based on compositions in diagrams a and c, at which observed dripwater Mg/Ca and Sr/Ca deviate from model calcite and dolomite recrystallization curves. G1 is Ca = 120 mg/L, Mg = 30 mg/L, Sr = 0.10 mg/L, Mg/Ca = 0.42 mol/mol, Sr/Ca = 0.38 mmol/mol. G3 is Ca = 120 mg/L, Mg = 10 mg/L, Sr = 0.06 mg/L, Mg/Ca = 0.14 mol/mol, and Sr/Ca = 0.23 mmol/mol. The K_D values for Mg and Sr are 0.023 and 0.12, respectively (median values for central Texas caves; Stern et al., 2005).

Ca (but not Mg/Ca) values observed in the summer at Natural Bridge Caverns for multiple reasons: (1) the first explanation would result in decreased Mg/Ca and Sr/Ca values, (2) the second explanation would require an increase in drip-water $^{87}\text{Sr}/^{86}\text{Sr}$ values to reflect an enhanced soil water contribution, but no such increases are observed, and (3) both explanations would cause changes in both Mg/Ca and Sr/Ca. Additionally, deviations from model curves cannot be accounted for by K_D values that might vary with calcite growth rate (Sr). Modeled Sr/Ca (and Mg/Ca) are only sensitive to variable K_D values at lower Ca concentrations (i.e., greater water–rock interactions), whereas the observed data deviates from the model curve at higher Ca concentrations. The limited sensitivity of the model to K_D values is, in part, a power of the modeling approach, as process curves can be constructed that are not sensitive to K_D values, which might not be well constrained. We cannot, however, explain the summer-exclusive excess Sr source at NBVC.

Model results further suggest several characteristics of the processes involved. Groups 1–3 dripwater can evolve from a similar soil–water composition (Fig. 8). The sequence of reactions (water–rock interaction followed by calcite precipitation), indicates that water–rock interaction occurs in the carbonate rock above the cave and PCP occurs within either the cave or vadose pores connected to the cave (Fig. 7). Groups 2 and 3 compositions that are displaced from the water–rock interaction trends are due to either interaction with host-rock minerals of distinct composition (Musgrove and Banner, 2004), or to relatively limited extents of PCP. The relative positions of drip-water compositions along the model trends reflect progressively increasing extents of water–rock interaction from Groups 2 and 3 to Group 1 (Fig. 8), consistent with drip-rate characteristics that indicate increasing water residence times from Groups 2 and 3 to Group 1. Group 1 drip-water compositions are non-responsive to variations

in water residence time (and thus water flux; Fig. 4), which is consistent with the lack of correlation between measures of water flux and dripwater compositions (Table 2), and suggests Group 1 dripwater is supplied from compositionally homogeneous vadose reservoir large enough to buffer variations in rainfall. Groups 2 and 3 dripwater are sensitive to, and thus have the potential to reflect, varying wet/dry conditions, on a sub-annual to annual timescale (Fig. 4). This is consistent with the more numerous and stronger correlations of Groups 2 and 3 between measures of water flux and dripwater compositions (Table 2).

5.2. Seasonal variation of Mg/Ca and Sr/Ca

Two results of this study indicate that seasonal controls dictate Group 1 dripwater Mg/Ca and Sr/Ca: (1) the consistent seasonal variations of elevated Mg/Ca and Sr/Ca in Group 1 dripwater during the cool, ventilated season and the opposite in the warm season when cave-air CO₂ is high (Figs. 3 and 6), and (2) model results indicating that PCP following water–rock interaction are the processes that likely account for the elevated Mg/Ca and Sr/Ca of Group 1 dripwater. Previous studies have inferred that seasonal changes in water flux through the vadose zone, driven by changes in rainfall, control dripwater Mg/Ca and Sr/Ca on seasonal time scales in several settings (Karmann et al., 2007; McDonald et al., 2007). In central Texas, however, interannual rainfall is extremely variable (Fig. 2), as exemplified by the rainfall record for the sampling interval (Fig. 6), and effective precipitation closely follows rainfall (Musgrove and Banner, 2004).

Seasonal ventilation of cave-air CO₂ has been shown to occur in several caves in this region, and to account for seasonal variations in calcite precipitation in both this and other caves (Banner et al., 2007; Cowan, 2010). Cool season, density-driven cave ventilation lowers cave-air CO₂ and enhances calcite precipitation (along the flow path prior to drip-water collection). Mg/Ca and Sr/Ca increase as calcite is precipitated due to the preferential partitioning of calcium into the mineral phase, which increases Mg and Sr concentrations relative to Ca. The occurrence of the highest Mg/Ca and Sr/Ca values in Group 1 dripwater is coincident with intervals when surface air density exceeds cave air density, and when cave-air CO₂ values are the lowest and calcite growth rates are highest (i.e., dark grey intervals in Fig. 6). This indicates that density-driven ventilation of cave air CO₂ is the mechanism controlling seasonal variations in Mg/Ca and Sr/Ca.

Further consistent with this mechanism, Group 1 dripwater Mg/Ca and Sr/Ca values fall between the annual minimum and maximum values during the transitional periods (i.e., light grey intervals in Fig. 6) when surface air fluctuates between being more and less dense than cave air. Interannual variability in cool season Mg/Ca and Sr/Ca maxima, however, do not correspond with physical or hydrologic parameters during the time period of this study. Higher resolution monitoring of cave-air CO₂ and cave and surface air temperature and density would likely resolve the mechanisms controlling this interannual variability.

Variability in dripwater Mg/Ca and Sr/Ca related to seasonal ventilation is consistent with a previous study at Natural Bridge Caverns and another cave in the region that documented seasonal dripwater $\delta^{13}\text{C}$ variations (Guilfoyle, 2006). Seasonal variations in dripwater $\delta^{13}\text{C}$ were observed in Group 2 (NBWS, NBF, NBEL) and Group 3 (NBCT) drip sites and were linked to seasonal decreases of cave-air CO₂ and enhanced CO₂ degassing from dripwater. Similar observations and conclusions were made in an Austrian cave (Spotl et al., 2005). Associated changes in dripwater Mg/Ca, however, were not observed in either case. The absence of corresponding $\delta^{13}\text{C}$ and Mg/Ca variations observed by Guilfoyle (2006) at Groups 2 and 3 sites suggests that either (1) CO₂ degasses from dripwater without forcing a sufficient amount of calcite precipitation to measurably affect drip-water Mg/Ca (Spotl et al., 2005), or (2) water–rock interaction is a dominant (Group 2) and influential (Group 3) control on Mg/Ca variability and interrupts the correlation between Mg/Ca and $\delta^{13}\text{C}$ variations. It is likely that Group 1 sites have seasonal variations in $\delta^{13}\text{C}$ in addition to the observed seasonal variations in Mg/Ca and Sr/Ca as this study has demonstrated that PCP is the dominant control at Group 1 drip sites. Neither Guilfoyle (2006) nor this study, however, has measured $\delta^{13}\text{C}$ for Group 1 drip sites.

There is no apparent reason for what causes ventilation-driven PCP to be a dominant control of dripwater Mg/Ca and Sr/Ca at Group 1, influential at Group 3 sites, and undetectable at Group 2 sites. We suggest that the degree of ventilation along the flow route might be a significant factor influencing the extent of PCP that can occur. Flow routes in which water flows across extensive surfaces (such as cave walls, flowstones, or large ceiling formations) can readily degas CO₂ and are likely more sensitive to fluctuations in cave air CO₂ than flow routes (such as those that pass through soda straws) that may be more prohibitive to CO₂ degassing. A possible hypothesis is that ventilation driven PCP variations are dominant and influential at Groups 1 and 3 drip sites, respectively, because of the type of ceiling formations (cave bacon, chandeliers, flowstone, fin shaped draperies; Table 4A) allow for degassing more readily than the ceiling formations (soda straws and short, stubby formations) that Group 2 drips fall from. This hypothesis is speculative, and a quantitative investigation is beyond the scope of this work.

6. IMPLICATIONS

6.1. Chemical indicator of annual lamina and speleothem bias

The seasonal Mg/Ca and Sr/Ca variations exhibited by Group 1 dripwaters may be recorded in speleothems and serve as chemical indicators of seasonal changes (Baker et al., 2008; Fairchild and Tremble, 2009). A similar study documented the presence of seasonal Mg/Ca and Sr/Ca variations in a speleothem underlying a drip with seasonal variations in Mg/Ca and Sr/Ca variations, illustrating the strong potential for seasonally resolved speleothem records (Mattey et al., 2010). Seasonal variations in dripwater Mg/Ca and Sr/Ca (in this study and Mattey et al., 2010) occur

independent of changes in water flux, making this potential for seasonal resolution in speleothems applicable for caves from the many regions that likely undergo seasonal ventilation (Banner et al., 2007; Baldini et al., 2008; James and Banner, 2009; Kowalczyk and Froelich, 2010). This process would allow for annual resolution of paleoclimate records in speleothems that may otherwise bear no physical evidence of annual lamina. The magnitude and timing of speleothem Mg/Ca and Sr/Ca fluctuations may serve as a proxy for seasonality in parameters that affect the density difference between the surface and cave, such as the seasonal timing of initial or final storm or the frequency or duration of storms that occur during the season when ventilation is highest and cave-air CO₂ is lowest.

Seasonal variations in dripwater Mg/Ca and Sr/Ca combined with observations of seasonal variations in calcite growth rate (Banner et al., 2007; Baldini et al., 2008) suggest that some speleothem records may be biased toward climate conditions for time periods during which the cave is ventilated. It is possible that speleothem records from

many temperate and high-latitude regions contain a seasonal bias towards higher than average Mg/Ca and Sr/Ca as more calcite growth occurs during ventilated seasons when dripwater Mg/Ca and Sr/Ca are higher (James and Banner, 2009). With slowed or no calcite growth during the non-ventilated season, lower Mg/Ca and Sr/Ca calcite would not be included in the record (Banner et al., 2007; Baldini et al., 2008).

6.2. Identifying controls on Mg/Ca and Sr/Ca variations

Different drip sites record different types of compositional variation. Our results are consistent with the findings that conduit-supplied drip sites have the potential to reflect short-term (sub-annual) rainfall variations whereas diffuse supplied drip sites have the potential to reflect more subdued, long-term rainfall variations (Karmann et al., 2007; McDonald et al., 2007; Fairchild and Tremble, 2009). In addition, we demonstrate that seasonally variable PCP related to cave-air CO₂ ventilation, and independent of

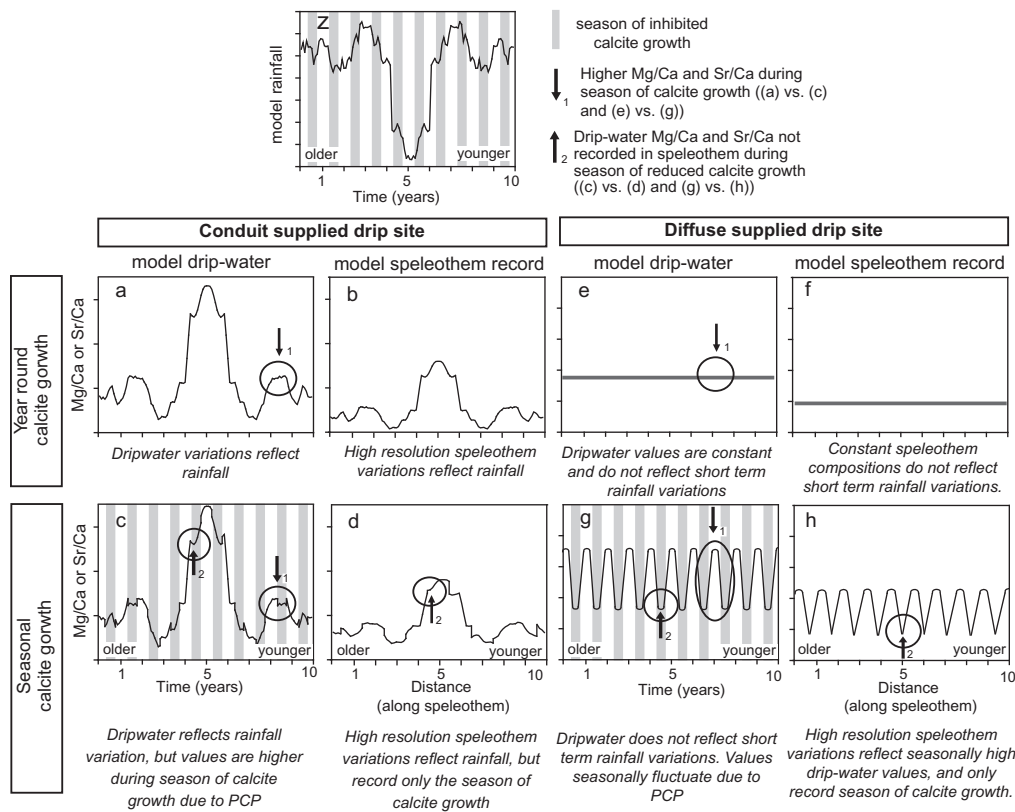


Fig. 9. Forward model showing potential dripwater and speleothem records (a–h) that would result from a given rainfall record (z) under conduit (a–d) and diffuse supplied (e–h) drip sites in caves with (c, d, g, h) and without (a, b, e, f) seasonal calcite growth variations. This model illustrates the link between high-frequency Mg/Ca and Sr/Ca patterns and the dripwater processes responsible for such variations. Arrow labeled “1” highlights that PCP causes seasonally higher dripwater Mg/Ca and Sr/Ca values, as seen by higher values in the dripwater with seasonal calcite growth variations relative to the dripwater with constant calcite growth rates (a vs. c, e vs. g). Arrow labeled “2” highlights that seasonally reduced calcite growth rates inhibit the preservation of dripwater Mg/Ca and Sr/Ca values that occur during that season, which results in the asymmetric Mg/Ca and Sr/Ca cycles (the troughs of high frequency Mg/Ca and Sr/Ca are truncated and compressed together) in the speleothem record (panel h) relative to the dripwater (panel g). Note that this model assumes that a given unit of distance along speleothem is equivalent to a year, and that variations in growth rate would determine the actual distance along a speleothem that corresponds to a year.

rainfall variations, can affect both conduit- and diffuse-supplied drip sites. Paleoclimate reconstructions should consider seasonal cave-air ventilation as a possible mechanism for high frequency speleothem Mg/Ca and Sr/Ca fluctuations.

Monitoring Mg/Ca and Sr/Ca variability in modern dripwater may provide insight into the processes that control dripwater, and thus speleothem, Mg/Ca and Sr/Ca variations. Monitoring studies, however, are time and resource intensive, and can only be conducted at caves that are readily and repeatedly accessible. It would be useful to infer information about the processes controlling dripwater composition without such accessibility. We suggest that the pattern of *high-frequency* speleothem Mg/Ca and Sr/Ca variations (as measured by such methods as laser ablation ICP-MS) might be indicative of controls that acted on dripwater compositions.

The results from our cave monitoring study are used to design a forward model that illustrates the types of speleothem variations that might result from varying controls on dripwater compositions and speleothem growth. For a given rainfall record, dripwater and speleothem Mg/Ca (or Sr/Ca) time series are modeled for various combinations of factors that influence dripwater compositions and speleothem growth (Fig. 9). We consider drip sites supplied by conduit and diffuse flow and caves with continuous and seasonal calcite growth. Forward modeling has previously been used to quantify speleothem $\delta^{18}\text{O}$ variability that might result from altering storage and discharge within a karst system (Baker and Bradley, 2010). Our model is different as we consider both storage and discharge parameters (in the form of conduit and diffuse flow) as well as continuous and seasonal speleothems growth. The objective is to provide a basis for interpreting paleo-dripwater controls from high frequency speleothem Mg/Ca and Sr/Ca variations.

For caves with continuous calcite growth, conduit-supplied drip sites will closely track rainfall variations (Fig. 9a), and diffuse-supplied drip sites will have more constant drip-water Mg/Ca and Sr/Ca values (Fig. 9e). Similarly, speleothems at conduit sites would exhibit short-term variation in accordance with the degree of past rainfall variability (Fig. 9b), and diffuse sites would exhibit consistent Mg/Ca and Sr/Ca values (Fig. 9f).

Diffuse-supplied drip sites affected by seasonal reductions of calcite growth will have dripwater compositions with seasonal Mg/Ca and Sr/Ca fluctuations (similar to Group 1 drip sites of this study; Fig. 9g). Conduit-supplied drip sites may or may not be affected by seasonal calcite growth variations (similar to Groups 3 and 2 drip sites, respectively). Conduit-supplied drip sites affected by seasonal calcite growth variations will exhibit elevated Mg/Ca and Sr/Ca during the season of calcite growth (arrow labeled “1”, Fig. 9c). Speleothems underlying diffuse drip sites will exhibit Mg/Ca and Sr/Ca fluctuations around a consistent mean. Note that the limited amount of calcite deposited during the season of reduced calcite growth would result in speleothem Mg/Ca and Sr/Ca cycles with truncated and compressed troughs (arrow labeled “2”, Fig. 9h). Speleothems supplied by conduit drip sites would

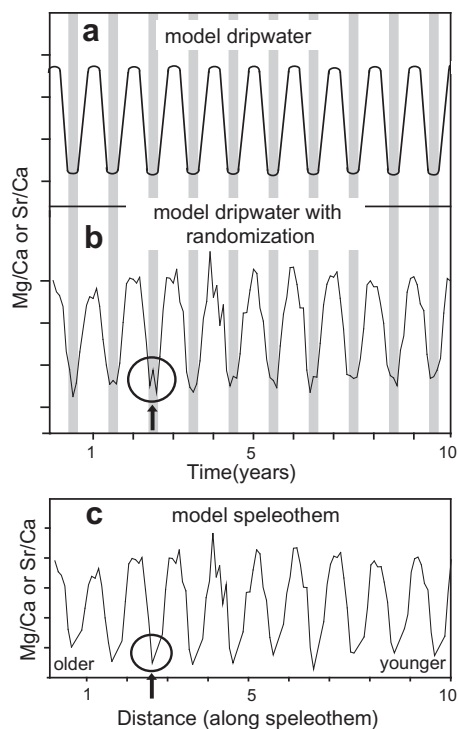


Fig. 10. (a) Conceptual diagram illustrating synthetic Mg/Ca or Sr/Ca variations from a diffuse flowpath supplied drip site affected by seasonal cave air CO_2 ventilation (same as Fig. 9g); (b) same as (a) with random error added by using a random number generator function; (c) synthetic speleothem record that would be deposited from (b). Note that this model assumes that a given unit of distance along speleothem is equivalent to a year, and that variations in growth rate would determine the actual distance along a speleothem that corresponds to a year.

exhibit Mg/Ca and Sr/Ca variations in accordance with the degree of past rainfall variability, but without a record of values that occurred during the season of reduced calcite growth (arrow labeled “2”, Fig. 9d).

Incorporating random variability to the forward model of dripwater Mg/Ca (or Sr/Ca) from a diffuse-supplied drip site affected by seasonal calcite growth provides a more realistic result (Fig. 10). The basic model (Fig. 9g) results from multiplying the mean Mg/Ca value of a given distribution by a coefficient >1 during the growing seasons, and by a coefficient <1 for the limited calcite growth seasons. Random variability is incorporated by creating a series of randomly generated numbers from the mean and one standard deviation of the prior distribution, and multiplying the series by the appropriate coefficient for the season. The resulting modeled speleothem record was created by omitting the interval for 2 of the 3 months that occur during the limited calcite growth season (Fig. 10).

We note the similarity between our modeled Mg/Ca (or Sr/Ca) record affected by seasonal reductions of calcite growth and published speleothem records that are interpreted to have seasonal lamina (Fig. 11; Roberts et al., 1998; Johnson et al., 2006). Similar features include (1) the high-frequency cyclical nature of Mg/Ca and Sr/Ca

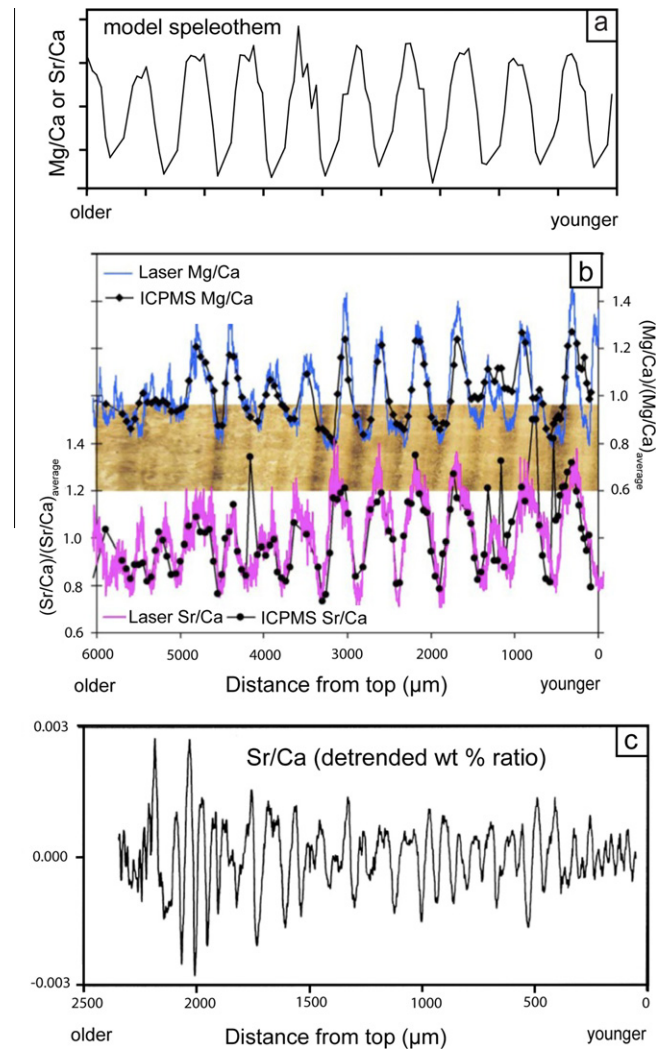


Fig. 11. (a) Synthetic speleothem record that would be deposited from a diffuse-supplied drip site affected by seasonal cave air CO_2 ventilation (same as Fig. 6c); (b) observed high-resolution speleothem Mg/Ca and Sr/Ca fluctuations from Johnson et al. (2006), and (c) Roberts et al. (1998).

variations, (2) truncation and compression of troughs of Mg/Ca and Sr/Ca cycles, and (3) variability of peak shape of Mg/Ca and Sr/Ca cycles, including irregular asymmetry and occasional sharp peaks and double peaks (Fig. 11). The Mg/Ca and Sr/Ca variations in these speleothem records are interpreted to reflect seasonal changes in water residence time (Roberts et al., 1998) and PCP (Johnson et al., 2006), as opposed to seasonal ventilation of cave-air CO_2 . Cave monitoring studies have demonstrated that the speleothem presented by Johnson et al. (2006) is from a cave (Heshang) that is strongly influenced by monsoonal rainfall variations, ventilated year round, and from beneath a drip site with a highly variable drip rate that is responsive to rainfall events (Hu et al., 2008). The similarity of the model-derived and observed speleothem records suggests that seasonal growth, either resulting from seasonal ventilation of cave-air CO_2 or strongly seasonal rainfall variations (the case in Heshang), results in a bias against the season of limited calcite growth.

The consistency between observed dripwater Mg/Ca and Sr/Ca variations in Texas (Group 1, Fig. 3), modeled speleothem variations, and observed speleothem variations from other studies (Fig. 11) provides strong evidence that high-frequency Mg/Ca and Sr/Ca can serve as a proxy for environmental changes on a seasonal scale. We demonstrate that seasonal ventilation of cave air CO_2 is responsible for seasonally variable calcite growth in this cave, but other mechanisms, such as strongly seasonal rainfall or cave air temperature, may also cause seasonally variable calcite growth. High frequency Mg/Ca and Sr/Ca variations are useful as an indicator of seasonal environmental changes, but, alone, are limited in their ability to identify the exact environmental mechanism responsible for the seasonality.

7. CONCLUSIONS

A 4-year dripwater monitoring study provides insights into the controls on cave dripwater Mg/Ca and Sr/Ca

variations. We identify three groups of dripwater sites based on inferred type of supplying flow path (diffuse vs. conduit), dripwater elemental and isotopic covariations, correlations between dripwater compositions (i.e., Mg/Ca, Sr/Ca, and $^{87}\text{Sr}/^{86}\text{Sr}$) and measures of water flux (i.e., rainfall and drip rate), and seasonal variation of dripwater Mg/Ca and Sr/Ca. We demonstrate that the covariation of Sr isotopes and Mg/Ca (and Sr/Ca) can be used to distinguish between Mg/Ca and Sr/Ca variations driven by water–rock interaction vs. prior calcite precipitation (PCP). Water–rock interaction (i.e., calcite or dolomite recrystallization) and seasonally variable PCP, which we distinguish between, can account for most dripwater compositions. Seasonally variable PCP (1) is caused by seasonal density-driven ventilation of cave-air CO_2 , (2) occurs independent of changes in water flux, and (3) results in seasonal variations of dripwater Mg/Ca and Sr/Ca at some drip sites. We construct a forward model to illustrate the types of high frequency speleothem Mg/Ca and Sr/Ca variations that would result from various combinations of controls on dripwater compositions.

Results of this study have multiple implications. Seasonal variations in dripwater Mg/Ca and Sr/Ca might be recorded in underlying speleothems and act as chemical indicators of seasonal laminae in caves that undergo seasonal ventilation of cave-air CO_2 . Paleoclimate reconstructions should consider seasonal cave-air ventilation as a possible mechanism for high frequency Mg/Ca and Sr/Ca fluctuations in speleothems. The combined observation of seasonally variable dripwater Mg/Ca and Sr/Ca (this study) and calcite growth rates (Banner et al., 2007), provides evidence that speleothems may be biased toward higher Mg/Ca and Sr/Ca values that reflect the season of enhanced calcite growth. Forward modeling demonstrates that patterns of high-frequency speleothem Mg/Ca and Sr/Ca values might provide insight into the controls of paleo-dripwater Mg/Ca and Sr/Ca, and thus improve interpretations of past climate of speleothems from caves for which multi-year cave monitoring is not possible.

ACKNOWLEDGMENTS

We thank the Wuest family and staff at Natural Bridge Caverns for access to the cave and weather station data. Scientific input and assistance in the field and laboratory were provided by Brian Vauter, Larry Mack, Eric James, Brian Cowan, Mike Osborne, Sarah Pierson, Amber Guilfoyle, and Lauren Greene. The manuscript benefited from comments provided by Kathleen Johnson and two anonymous reviewers. This article was made possible by EPA STAR fellowship number FP916874. Its contents are solely the responsibility of the fellow and do not necessarily represent the official views of the EPA. Support was also provided for by the National Science Foundation's P2C2 Program (ATM-0823665) and GK-12 and RET supplemental Program (DGE-0638740), the Jackson School of Geosciences, Texas Water Resources Institute, UT-Austin's Geology Foundation and Environmental Science Institute, the Geological Society of America, and the South Central Texas Geological Society.

APPENDIX A. SUPPLEMENTARY DATA

Supplementary data associated with this article can be found, in the online version, at doi:10.1016/j.gca.2011.03.025.

REFERENCES

- Baker A. and Bradley C. (2010) Modern stalagmite $\delta^{18}\text{O}$: instrumental calibration and forward modeling. *Global Planetary Change* **71**, 201–206.
- Baker A., Smith C. L., Jex C., Fairchild I. J., Genty D. and Fuller L. (2008) Annually laminated speleothems: a review. *Int. J. Speleol.* **37**, 193–206.
- Baldini J. U. L., McDermott F. and Fairchild I. J. (2006) Spatial variability in cave drip water hydrochemistry: implications for stalagmite paleoclimate records. *Chem. Geol.* **235**, 290–304.
- Baldini J. U. L., McDermott F., Hoffmann D. L., Richards D. A. and Clipson N. (2008) Very-high frequency and seasonal cave atmosphere P_{CO_2} variability: Implications for stalagmite growth and oxygen isotope-based paleoclimate records. *Earth Planet. Sci. Lett.* **272**, 118–129.
- Banner J. L. and Kaufman J. (1994) The isotopic record of ocean chemistry and diagenesis preserved in non-luminescent brachiopods from Mississippian carbonate rocks, Illinois and Missouri. *Geol. Soc. Am. Bull.* **106**, 1074–1082.
- Banner J. L., Musgrove M., Edwards R. L., Asmerom Y. and Hoff J. A. (1996) High-resolution temporal record of Holocene groundwater chemistry: tracing links between climate and hydrology. *Geology* **24**, 1049–1052.
- Banner J. L., Guilfoyle A., James E., Stern L. A. and Musgrove M. (2007) Seasonal variations in modern speleothem calcite growth in Central Texas, USA. *J. Sed. Res.* **77**, 615–622.
- Boch R. and Spotl C. (2008) The origin of lamination in stalagmites from Katerloch Cave, Austria: Towards a seasonality proxy. *PAGES News* **16**, 1–22.
- Cooke M. J., Stern L. A., Banner J. L. and Mack L. E. (2007) Evidence for the silicate source of relict soils on the Edwards Plateau, central Texas. *Quatern. Res.* **67**, 275–285.
- Cowan B. D. (2010) Temporal and spatial variability of cave-air carbon dioxide in Central Texas, USA. MS thesis, The University of Texas at Austin.
- Elliott, W. R. and Veni, G. (eds.) (1994) *The Caves and Karst of Texas in NSS Convention Guidebook*. National Speleological Society, Huntsville, AL.
- Fairchild I. J. and Tremble P. C. (2009) Trace elements in speleothems as recorders of environmental change. *Quatern. Sci. Rev.* **28**, 449–468.
- Genty D. and Deflandre G. (1998) Drip flow variations under a stalactite of the Pere Noel cave (Belgium). Evidence of seasonal variations and air pressure constraints. *J. Hydrol.* **211**, 208–232.
- Guilfoyle A. (2006) Temporal and spatial controls on cave water and speleothem calcite isotopic and elemental chemistry. MS thesis, The University of Texas at Austin.
- Hu C., Henderson G. M., Huang J., Chen Z. and Johnson K. R. (2008) Report of a three-year monitoring programme at Heshang Cave, Central China. *Int. J. Speleol.* **37**, 143–151.
- James E. and Banner J. L. (2009) Factors promoting preservation bias in speleothem growth. In *Proceedings 15th International Congress of Speleology, Kerrville, Texas* (ed. W.B. White). International Union of Speleology, p. 1025.
- Jo K., Woo K. S., Hong G. H., Kim S. H. and Suk B. C. (2010) Rainfall and hydrological controls on speleothem geochemistry during climatic events (droughts and typhoons): an example

- from Seopdong Cave, Republic of Korea. *Earth Planet. Sci. Lett.* **295**, 441–450.
- Johnson K. R., Hu H., Belshaw N. S. and Henderson G. M. (2006) Seasonal trace element and stable isotope variations in a Chinese speleothem: the potential for high-resolution paleomonsoon reconstruction. *Earth Planet. Sci. Lett.* **244**, 394–407.
- Karmann I., Cruz F. W., Oduvaldo V. J. and Burns S. J. (2007) Climate influence on geochemistry parameters of waters from Santana–Perolas cave system, Brazil. *Chem. Geol.* **244**, 232–247.
- Kowalczyk A. J. and Froelich P. N. (2010) Cave air ventilation and CO₂ outgassing by radon-222 modeling: How fast do caves breathe? *Earth Planet. Sci. Lett.* **289**, 209–219.
- Maclay R. W. and Small T. A. (1983) Hydrostratigraphic subdivisions and fault barriers of the Edwards aquifer, south-central Texas, USA. *J. Hydrol.* **61**, 127–146.
- Mattey D. P., Fairchild I. J., Atkinson T. C., Latin J. P., Ainsworth M. and Durrell R. (2010) Gibraltar and trace elements in modern speleothem from St Michaels Cave, Seasonal microclimate control of calcite fabrics, stable isotopes. *Geol. Soc. Lond. Spec. Publ.* **336**, 323–344.
- McDonald J., Drysdale R., Hill D., Chisari R. and Wong H. (2007) The hydrochemical response of cave drip-waters to sub-annual and inter-annual climate variability, Wombeyan Caves, SE Australia. *Chem. Geol.* **244**, 605–623.
- Mihealsick C. A., Banner J. L., Musgrove M., James E. W., Guilfoyle A. L. and Pierson S. J. (2004) Applications of Mg/Ca and Sr/Ca ratios to groundwater evolution in the Edwards Aquifer of central Texas. *Geol. Soc. Am. Abstr. Prog.* **36**, 327–328.
- Musgrove M. and Banner J. L. (2004) Controls on the spatial and temporal variability of vadose dripwater geochemistry: Edwards aquifer, central Texas. *Geochim. Cosmochim. Acta* **68**, 1007–1020.
- Oetting G. C. (1995) Evolution of fresh and saline groundwaters in the Edwards aquifer, central Texas: geochemical and isotopic constraints on processes of fluid–rock interaction and fluid mixing. Dissertation, The University of Texas at Austin.
- Pape J. R., Banner J. L., Mack L. E., Musgrove M. and Guilfoyle A. (2010) Controls on oxygen isotope variability in precipitation and cave dripwaters, central Texas, USA. *J. Hydrol.* **385**, 203–215.
- Roberts M. S., Smart P. L. and Baker A. (1998) Annual trace element variations in a Holocene speleothem. *Earth Planet. Sci. Lett.* **154**, 237–246.
- Small T. A. and Hanson J. A. (1994) Geologic framework and hydrogeologic characteristics of the Edwards Aquifer outcrop, Comal County, Texas, US Geol. Survey Water Res. Invest. Rep. 94–4117.
- Smart P. L. and Friederich H. (1986) Water movement and storage in the unsaturated zone of a maturely karstified aquifer, Mendip Hills, England. In *Proceedings of the Conference on Environmental Problems in Karst Terrains and their Solutions*. National Water Wells Association, Bowling Green, KY, pp. 57–87.
- Spotl C., Fairchild I. J. and Tooth A. F. (2005) Cave air control on dripwater geochemistry, Obir Caves (Austria): Implications for speleothem deposition in dynamically ventilated caves. *Geochim. Cosmochim. Acta* **69**, 2451–2468.
- Stern L. A., Banner J. L., Cowan B., Copeland E. A., Mickler P., Guilfoyle A., James E. W., Musgrove M. and Mack L. E. (2005) Trace element variations in speleothem calcite: influence of non-environmental factors. *Geol. Soc. Am. Abstr. Prog.* **193**, 7.
- Wong C. and Banner J. L. (2010) Response of cave air CO₂ and dripwater to brush clearing. *J. Geophys. Res.* **115**, G04018.

Associate editor: Miryam Bar-Matthews